LBL--25768

DE89 013371

# Pressure-driven Brine Migration in a Salt Repository

**Y. Hwang, P. L. Chambré, T. H. Pigford, and W. W.-L. Lee**

**Department of Nuclear Engineering**
**University of California**
**and**
**Earth Sciences Division,**
**Lawrence Berkeley Laboratory**
**1 Cyclotron Road**
**Berkeley, CA 94720**

**January 1989**



*Work supported in part by the Director, Office of Civilian Radioactive Waste Management, Office of Systems Integration and Regulations, Licensing and Compliance Division, of the U. S. Department of Energy under contract DE-AC03-76SF00098.*

**The authors invite comments and would appreciate being notified of any errors in the report.**

**T. H. Pigford**
**Department of Nuclear Engineering**
**University of California**
**Berkeley, CA 94720**

## Contents



## List of Figures

## 1. Introduction

The traditional view is that salt is the ideal rock for isolation of nuclear waste because it is "dry" and probably "impermeable." The existence of salt through geologic time is *prima facie* evidence of such properties. Experiments and experience at potential salt sites for geologic repositories have indicated that while porosity and permeability of salt are low, the salt may be saturated with brine.[1] If this hypothesis is correct, then it is possible to have brine flow due to pressure differences within the salt. If there is pressure-driven brine migration in salt repositories then it is paramount to know the magnitude of such flow because inward brine flow would affect the corrosion rate of nuclear waste containers and outward brine flow might affect radionuclide transport rates.

Brine exists in natural salt as inclusions in salt crystals and in grain boundaries. Brine inclusions in crystals move to nearby grain boundaries when subjected to a temperature gradient, because of temperature-dependent solubility of salt. Brine in grain boundaries moves under the influence of a pressure gradient.[1,2] When salt is mined to create a waste repository, brine from grain boundaries will migrate into the rooms, tunnels and boreholes because these cavities are at atmospheric pressure. After a heat-emitting waste package is emplaced and backfilled, the heat will impose a temperature gradient in the surrounding salt that will cause inclusions in the nearby salt to migrate to grain boundaries within a few years, adding to the brine that was already present in the grain boundaries.

Until the heated salt immediately adjacent to the waste package has consolidated, brine can accumulate in the annular space between the container and the emplacement hole wall. This brine movement is due to the difference in brine pressure within the salt and the lower pressure in the borehole. Similarly, the lithostatic pressure of the surrounding salt, augmented by the compressive stresses of heating, causes salt to creep against the waste container. Brandshaug[3] predicts that, within a few years after emplacement of a high-level waste container, creep closure of the salt will result in consolidated salt completely enclosing the waste container.

After the consolidation of salt around the waste package, neglecting the consumption of brine by container corrosion, brine in grain boundaries near the waste package can only migrate outward into the surrounding salt, under the influence of pressure gradients caused by transient heating of the salt. Hot salt near the waste package expands against the waste package and surrounding salt, creating high compressive stresses near the waste package and resulting in pressure above the lithostatic pressure. Brine pressure further increases because grain-boundary brine expands more than does the salt and this increased pressure gradient causes brine to flow outward into the cooler salt.[4] Outward flow of brine relieves the pressure gradient on the fluid, which finally relaxes to near-lithostatic pressure. If the waste containers are failed by corrosion or cracking, this outward brine movement can become a mechanism for radionuclide transport. To determine

the extent to which advection by brine in grain boundaries is an important transport mechanism for released radionuclides, it is necessary to estimate the time-dependent migration of brine after salt consolidation.

The formulation of brine movement with salt as a thermoelastic porous medium, in the context of the continuum theory of mixtures, was first published by McTigue.[2] Chambré obtained the analytic solutions presented below to the governing equations for a spherical-equivalent waste form and to the coupled radionuclide transport problem, driven by thermoelastic effects. Elsewhere we have presented numerical results obtained from this theory.[5,6] In this report we show the mathematical details and discuss the results predicted by this analysis.

## 2. Analysis

In this report we deal with pressure-driven flow, and we must first define brine pressure. We define the relative pore pressure, $P$, of brine as the absolute pore pressure less the undisturbed, far-field pore pressure of brine which is approximated by lithostatic pressure. Consider point A on the wall of a borehole in a repository in salt (Figure 1). Before consolidation, the borehole is open to the atmosphere and the pressure at A is atmospheric, so the relative pressure is a negative quantity. At point B, some distance inside the salt, brine in grain boundaries is at a higher pressure. If Darcy's Law is valid for motion of grain-boundary brine, then the higher pressure at B would drive fluid from B to A. After consolidation, the boundary condition at A will become one of zero mass flux, rather than one of constant pressure. Now pressure gradients in the same regions can result in brine motion back into the salt.

The Darcy velocity can be written as

$$v(r,t) = -\frac{k}{\mu}\frac{\partial P}{\partial r} \tag{1}$$

where $P$ is the relative pore pressure [M $L^{-1}t^{-2}$],
$r$ is the distance variable [L],
$k$ is the permeability [$L^2$],
$\mu$ is the fluid viscosity [M $L^{-1}t^{-1}$].

To obtain an expression for $\frac{\partial P}{\partial r}$, we treat the salt as a linear thermoelastic solid. McTigue[2] derived the following expression, written here for salt surrounding an assumed spherical waste solid,

$$\frac{\partial P}{\partial t} = c\frac{1}{r^2}\frac{\partial}{\partial r}\left(r^2\frac{\partial P}{\partial r}\right) + b'\frac{\partial \theta}{\partial t}, \quad t > 0, r > a \tag{2}$$

where $\theta(r,t)$ is the relative temperature, actual minus ambient [T],
$a$ is the radius of spherical-equivalent waste package [L], and
$b'$, $c$ are constants which are functions of material properties

$$b' = \frac{4GB(1+\nu_u)}{9(1-\nu_u)}\left[\alpha_s' + \frac{B(1-\nu)(1+\nu_u)}{2(\nu_u-\nu)}\phi_0(\alpha_f - \alpha_s')\right] \tag{2a}$$

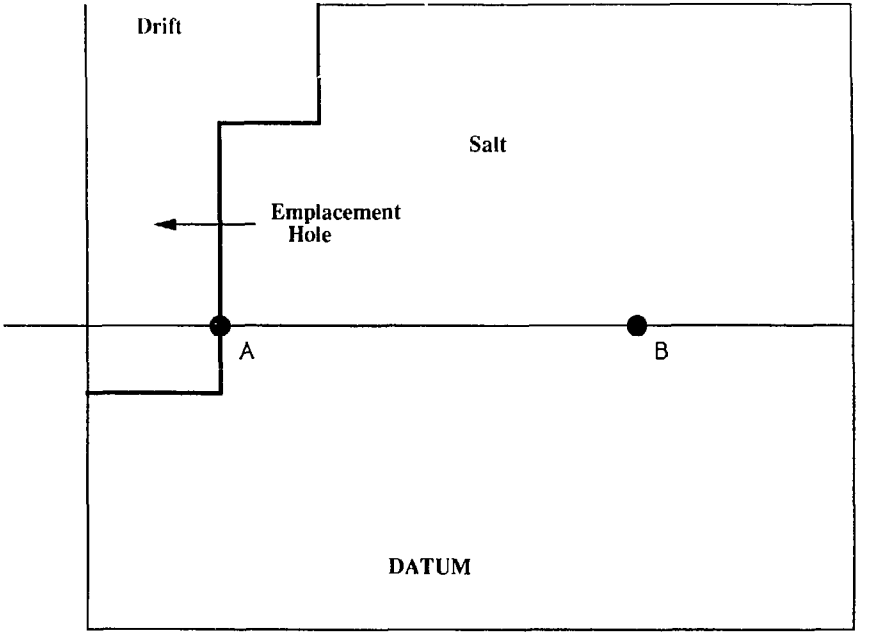


Figure 1. Elevation Schematic, Open Borehole

$$c = \frac{k}{\nu}\frac{2G(1-\nu)}{1-2\nu}\left[\frac{B^2(1-2\nu)(1+\nu_u)^2}{9(1-\nu)(\nu_u-\nu)}\right] \tag{2b}$$

where $G$ is the shear modulus [M $L^{-1}t^{-2}$]

$\nu$ is Poisson's ratio for the solid phase

$\nu_u$ is the undrained Poisson's ratio

$\phi_0$ is the reference porosity

$\alpha_f$ is the fluid-phase thermal expansion coefficient [$T^{-1}$]

$\alpha_s''$ is the second cubical thermal expansion coefficient of the solid [$T^{-1}$], and

$B$ is the pore-pressure modulus, where

$$\frac{1}{B} = 1 + \phi_0\frac{K(1-K_f/K_s'')}{K_f(1-K/K_s')}$$

in which $K$ is the bulk modulus [M $L^{-1}t^{-2}$], and

the subscripts $f$ and $s$ refer to the fluid phase and solid phase, respectively.

Equation (2) states that the variation in pore pressure is due primarily to the change of relative temperature. The derivation of (2) is given in McTigue[2] and not repeated here. The major assumptions in the derivation are

- The system is linearized.
- Thermal convection is neglected.
- Material properties are constant with temperature. Thus (2) is only valid for small temperature changes.
- The porous material is homogenous.

We present first the derivation of the temperature history around a waste package and then the solution to the above equations for two cases.

## 2.1 Temperature Field

According to (2), the pressure field response is due primarily to the change of temperature, on the right-hand-side of (2). In this section we obtain an analytic expression for the time derivative of temperature.

The governing equation for the temperature profile is

$$\frac{\partial\theta}{\partial t} - \frac{\kappa}{r^2}\frac{\partial}{\partial r}\left(r^2\frac{\partial\theta}{\partial r}\right) = 0, \qquad r > a, t > 0 \tag{3}$$

where $\kappa$ is the thermal diffusivity [$L^2/T$].

We use a known thermal decay rate as a boundary condition for solving (3)

$$-\lambda\frac{\partial\theta}{\partial r}\Big|_{r=a} = Q_0 f(t) \tag{4}$$

where

$\lambda$ is the thermal conductivity [M L $t^{-3}T^{-1}$],

$Q_o$ is the initial heat flux of the waste package [$M/t^3$], and

$f(t)$ is a known time history of the normalized heat flux of the waste package.

The other side conditions are

$$\theta(\infty, t) = 0, \qquad t > 0 \tag{5}$$

$$\theta(r, 0) = 0, \qquad r > a \tag{6}$$

To solve (3), (4), (5) and (6) let

$$V(r, t) = r\theta(r, t) \tag{7}$$

and substitute into (3)

$$\frac{\partial V}{\partial t} - \kappa \frac{\partial^2 V}{\partial r^2} = 0, \qquad r > a, t > 0 \tag{8}$$

Taking the Laplace transform of (8)

$$s\tilde{V}(r, s) - \kappa \frac{\partial^2 \tilde{V}}{\partial r^2} = 0, \qquad r > a \tag{9}$$

and using (5) obtain

$$\tilde{V}(r, s) = A_1 \exp\left\{-\sqrt{\frac{s}{\kappa}} r\right\} \tag{10}$$

Taking the Laplace transform of (4) we get

$$\left(-\frac{\partial \tilde{V}}{r} + \frac{\tilde{V}}{r}\right)\Bigg|_{r=a} = \theta_o \tilde{f}(s) \tag{11}$$

where

$$\theta_o = \frac{Q_o a}{\lambda} \tag{12}$$

Applying the Laplace Transform of (6) and (11) to (10) we get

$$A_1 \sqrt{\frac{s}{\kappa}} \exp\left\{-\sqrt{\frac{s}{\kappa}} a\right\} + \frac{1}{a} A_1 \exp\left\{-\sqrt{\frac{s}{\kappa}} a\right\} = \theta_o \tilde{f}(s) \tag{13}$$

$A_1$ is evaluated to be

$$A_1 = \frac{\theta_o \tilde{f}(s)}{\sqrt{\frac{s}{\kappa}} + \frac{1}{a}} \exp\left\{\sqrt{\frac{s}{\kappa}} a\right\} \tag{14}$$

and

$$\tilde{V} = \frac{\theta_o \sqrt{\kappa}}{\sqrt{s} + \sqrt{\alpha}} \tilde{f}(s) \exp\left\{-\sqrt{\frac{s}{\kappa}} (r - a)\right\} \tag{15}$$

where $\alpha = \kappa/a^2$. Using the inverse Laplace transform[7]

$$L^{-1}\left[\frac{\exp\{-\sqrt{\alpha s}\}}{\sqrt{s}+\sqrt{\alpha}}\tilde{f}(s)\right] = \int_0^t \left[\frac{1}{\sqrt{\pi\tau}}\exp\left\{\frac{-\varrho}{4\tau}\right\} - \sqrt{\alpha}\exp\{\sqrt{\alpha\varrho}+\alpha\tau\}\operatorname{erfc}\left\{\frac{1}{2}\sqrt{\frac{\varrho}{\tau}}+\sqrt{\alpha\tau}\right\}\right] f(t-\tau)d\tau \tag{16}$$

where

$$\varrho = \frac{(r-a)^2}{\kappa} \tag{17}$$

in (15) we obtain the salt temperature profile

$$\theta = \frac{V(r,t)}{r}$$

$$= \frac{\theta_o\sqrt{\kappa}}{r}\int_0^t f(t-\tau)\left[\frac{1}{\sqrt{\pi\tau}}\exp\left\{\frac{-(r-a)^2}{4\kappa\tau}\right\} - \sqrt{\frac{\kappa}{a^2}}\exp\left\{\frac{(r-a)}{a}+\frac{\kappa\tau}{a^2}\right\}\operatorname{erfc}\left\{\frac{1}{2}\frac{\tau-a}{\sqrt{\kappa\tau}}+\sqrt{\frac{\kappa\tau}{a^2}}\right\}\right]d\tau \tag{18}$$

and the relative temperature at the waste package surface can be evaluated by

$$\theta\Big|_{r=a} = \frac{\theta_o\kappa}{a^2}\int_0^t f(t-\tau)\left[\sqrt{\frac{a^2}{\pi\kappa\tau}} - \exp\left\{\frac{\kappa\tau}{a^2}\right\}\operatorname{erfc}\left\{\sqrt{\frac{\kappa\tau}{a^2}}\right\}\right]d\tau \tag{19}$$

When given a time-history of heat flux from a waste package, (19) allows us to obtain the temperature at the waste package surface and the time derivative of (18) gives us the source term for (2).

We use different initial and boundary conditions for the pore pressure to solve two different cases.

### 2.2 Case 1: Open Borehole

In this case the borehole or the emplacement room or drift is assumed to stay open for the duration of the analysis. The initial condition

$$P(r,0) = 0, \qquad r > a \tag{20}$$

and the boundary conditions

$$P(a,t) = -p_o \qquad t > 0 \tag{21}$$

where $p_o$ = lithostatic pressure minus atmospheric pressure

$$\lim_{r\to\infty} P(r,t) = 0 \qquad t > 0 \tag{22}$$

form the sufficient set to solve (2).

Let

$$W(r,t) = rP(r,t) \tag{23}$$

and substitute into (2), (20), (21) and (22) resulting in

$$\frac{\partial W}{\partial t} - c\frac{\partial^2 W}{\partial r^2} = b' r \frac{\partial \theta(r,t)}{\partial t} \tag{24}$$

$$W(r,0) = 0 \tag{25}$$

$$W(a,t) = -ap_o \tag{26}$$

$$\lim_{r\to\infty} \frac{W(r,t)}{r} = 0 \tag{27}$$

Taking the Laplace transform of (24) we have

$$s\tilde{W}(r,s) - W(r,0) = c\frac{\partial^2 \tilde{W}}{\partial r^2} + b' r(s\tilde{\theta}(r,s) - \theta(r,0)) \tag{28}$$

Using (25), (26), (28) and the Laplace Transform of (18) and (27) we have

$$\tilde{W}(r,s) = A_2 \exp\left\{-\sqrt{\frac{s}{c}}r\right\} + \frac{b'\theta_o\sqrt{\kappa}}{(1-R^2)(\sqrt{s}+\sqrt{\alpha})}\tilde{f}(s)\exp\left\{-\sqrt{\frac{s}{\kappa}}(r-a)\right\} \tag{29}$$

where

$$R^2 = c/\kappa \tag{30}$$

Taking the Laplace transform of (26) and evaluating (29) at $r = a$, we get

$$\tilde{W}(a,s) = A_2 \exp\left\{-\sqrt{\frac{s}{c}}a\right\} + \frac{b'\theta_o\sqrt{\kappa}}{(1-R^2)(\sqrt{s}+\sqrt{\alpha})}\tilde{f}(s) = -\frac{ap_o}{s} \tag{31}$$

and the constant $A_2$ can be evaluated as

$$A_2 = -\frac{ap_o}{s}\exp\left\{\sqrt{\frac{s}{c}}a\right\} - \frac{b'\theta_o\sqrt{\kappa}}{(1-R^2)(\sqrt{s}+\sqrt{\alpha})}\tilde{f}(s)\exp\left\{\sqrt{\frac{s}{c}}a\right\} \tag{32}$$

Then the solution by taking the inverse Laplace transform is

$$P(r,t) = -\frac{p_o}{r/a}\mathrm{erfc}\left\{\frac{r/a-1}{2R\sqrt{\alpha t}}\right\} + \frac{rb'\theta_o\sqrt{\kappa}}{(1-R^2)}\int_0^t f(t-\tau)\Upsilon(r,\tau)d\tau \tag{33}$$

where

$$\Upsilon(r,t) = \frac{1}{\sqrt{\pi t}}\left[\exp\left\{\frac{-(\frac{r}{a}-1)^2}{4\alpha t}\right\} - \exp\left\{\frac{-(\frac{r}{a}-1)^2}{4R^2\alpha t}\right\}\right]$$
$$- \sqrt{\alpha}\left[\exp\left\{(\frac{r}{a}-1)+\alpha t\right\}\mathrm{erfc}\left\{\frac{\frac{r}{a}-1}{2\sqrt{\alpha t}}+\sqrt{\alpha t}\right\} - \exp\left\{\frac{\frac{r}{a}-1}{R}+\alpha t\right\}\mathrm{erfc}\left\{\frac{\frac{r}{a}-1}{2R\sqrt{\alpha t}}+\sqrt{\alpha t}\right\}\right] \tag{34}$$

Using the differentiated form of (33) in (1) we obtain the Darcy velocity at the surface of a spherical waste package

$$v(a,t) = -\frac{kp_o}{\mu}\left[\frac{1}{\sqrt{\pi R^2 \kappa t}} + \frac{1}{a}\right] - \frac{kb'\theta_o}{a\mu(1+R)R}\left\{f(0)e^{\alpha t}\mathrm{erfc}\sqrt{\alpha t} + \int_0^t f'(\tau)(1-u(t-\tau))d\tau\right\} \tag{35}$$

where

$$u(t) = 1 - e^{\alpha t}\mathrm{erfc}\sqrt{\alpha t} \tag{36}$$

The cumulative brine flow $Q$ [$L^3$] through the waste sphere/salt interface can be calculated with

$$Q(t) = 4\pi a^2 \int_0^t v(a,\tau)d\tau \tag{37}$$

### 2.3 Case 2: Consolidated Salt

In this case salt creep closes the air gap between the waste package and the rock salt, in a matter of days to months after the emplacement of the waste package.[7] Thereafter, neglecting the consumption of brine by container corrosion, brine in grain boundaries faces an impermeable boundary where an air gap had existed in Case 1, and thus brine near the waste package can only migrate outward into the surrounding salt, under the influence of pressure gradients caused by transient heating of the salt. Hot salt near the waste package expands against the waste package and surrounding salt, resulting in high compressive stresses near the waste package. Grain-boundary brine expands more than does the salt and further increases the local presssure and pressure gradients that cause brine to flow outward into the cooler salt. Such outward flow of brine relieves the pressure gradient on the fluid, which finally relaxes to near-lithostatic pressure.

The governing equation (2) and the initial condition (20) remain the same. The boundary conditions are now

$$\lim_{r\to\infty} P(r,t) = 0 \qquad t > 0 \tag{38}$$

$$\left.\frac{\partial P(a,t)}{\partial r}\right|_{r=a} = 0, \qquad t > 0 \tag{39}$$

This set of initial and boundary conditions differs from the set for the open borehole case by the replacement of (21) with (39).

To solve this set of equations first set

$$W(r,t) = rP(r,t) \tag{40}$$

and substitute into (2) resulting in

$$\frac{\partial W}{\partial t} = c\frac{\partial^2 W}{\partial r^2} + b'r\frac{\partial P(r,t)}{\partial t}, \quad t > 0, r > a \tag{41}$$

Taking the Laplace transform of (41)

$$s\tilde{W}(r,s) - W(r,0) - c\frac{\partial^2 \tilde{W}}{\partial r^2} = b'r(s\tilde{\theta}(r,s) - \theta(r,0)) \tag{42}$$

From the side conditions (20) and the initial condition (6) of the temperature problem and using (15) with the Laplace Transform of (7) in (42) we have

$$\tilde{W}(r,s) - \frac{c}{s}\frac{\partial^2 \tilde{W}}{\partial r^2} = b'\frac{\theta_o\sqrt{\kappa}}{\sqrt{s}+\sqrt{\alpha}}\tilde{f}(s)\exp\left\{-\sqrt{\frac{s}{\kappa}}(r-a)\right\} \tag{43}$$

Using the side condition (38), the homogeneous solution to (43) is

$$\tilde{W}_h = A_3\exp\left\{-\sqrt{\frac{s}{c}}r\right\} \tag{44}$$

and the particular solution is

$$\tilde{W}_p = \frac{b'\theta_o}{(1-R^2)(q_1+1/a)}\tilde{f}(s)\exp\left\{-\sqrt{\frac{s}{\kappa}}(r-a)\right\} \tag{45}$$

where $q_1 = \sqrt{s/\kappa}$

Combining the homogeneous and particular solutions

$$\tilde{W}(r,s) = A_3\exp\left\{-\sqrt{\frac{s}{c}}r\right\} + \frac{b'\theta_o}{(1-R^2)(q_1+1/a)}\tilde{f}(s)\exp\left\{-\sqrt{\frac{s}{\kappa}}(r-a)\right\} \tag{46}$$

We use (39) to evaluate the constant $A_3$

$$\frac{\partial P}{\partial r}\Big|_{r=a} = \frac{\partial \frac{W}{r}}{\partial r}\Big|_{r=a} = \frac{1}{a}\frac{\partial W}{\partial r}\Big|_{r=a} - \frac{1}{a^2}W(a,t) = 0 \tag{47}$$

Taking the Laplace transform of (47)

$$\frac{1}{a}\frac{\partial \tilde{W}(r,s)}{\partial r}\Big|_{r=a} - \frac{1}{a^2}\tilde{W}(a,s) = 0 \tag{48}$$

and differentiating (46)

$$\frac{\partial \tilde{W}(r,s)}{\partial r}\Big| = -A_3\sqrt{\frac{s}{c}}\exp\left\{-\sqrt{\frac{s}{c}}a\right\} - \frac{b'\theta_o}{(1-R^2)(q_1+1/a)}\sqrt{\frac{s}{\kappa}}\tilde{f}(s) \tag{49}$$

Multiplying both sides of (48) by $a^2$ and substituting (49) and (46) into (48), we can evaluate $A_3$

$$-aA_3\sqrt{\frac{s}{c}}\exp\left\{-\sqrt{\frac{s}{c}}a\right\} - \frac{b'\theta_o a}{(1-R^2)(q_1+1/a)}\sqrt{\frac{s}{\kappa}}\tilde{f}(s) - A_3\exp\left\{-\sqrt{\frac{s}{c}}a\right\} - \frac{b'\theta_o}{(1-R^2)(q_1+1/a)}\tilde{f}(s) = 0 \tag{50}$$

$$A_3 = \frac{-b'\theta_o}{(1/a + \sqrt{s/c})(1-R^2)} \tilde{f}(s) \exp\left\{ \sqrt{\frac{s}{\kappa}} \frac{a}{R} \right\} \tag{51}$$

Then

$$\tilde{W}(r,s) = -\frac{b'\theta_o}{(1-R^2)(\sqrt{\frac{s}{\kappa}} + \frac{1}{a})} \tilde{f}(s) \exp\left\{ -\sqrt{\frac{s}{\kappa}}(r-a) \right\} - \frac{b'\theta_o}{(1-R^2)(\sqrt{\frac{s}{c}} + \frac{1}{a})} \tilde{f}(s) \exp\left\{ -\frac{\sqrt{\frac{s}{\kappa}}}{R}(r-a) \right\} \tag{52}$$

(52) can be written as

$$\tilde{W}(r,s) = \delta \frac{\tilde{f}(s)}{\sqrt{s} + \sqrt{\alpha}} \exp\left\{ -\sqrt{\beta s} \right\} - R\delta \frac{\tilde{f}(s)}{\sqrt{s} + \sqrt{w}} \exp\left\{ -\sqrt{\gamma s} \right\} \tag{53}$$

where

$$\delta = \frac{b'\sqrt{\kappa}\theta_o}{1-R^2}, \qquad \beta = \frac{(r/a-1)^2}{\alpha}$$

$$w = \frac{c}{a^2} = \alpha R^2, \qquad \gamma = \frac{(r/a-1)^2}{\alpha R^2}$$

Using the inverse Laplace transform[7]

$$L^{-1}\left[ \frac{1}{\sqrt{s} + \sqrt{\alpha}} \exp\left\{ -\sqrt{\beta s} \right\} \right] = \frac{1}{\sqrt{\pi t}} \exp\left\{ \frac{-\beta}{4t} \right\} - \sqrt{\alpha} \exp\left\{ \sqrt{\alpha\beta} + \alpha t \right\} \operatorname{erfc}\left\{ \frac{1}{2}\sqrt{\frac{\beta}{t}} + \sqrt{\alpha t} \right\} \tag{54}$$

and the convolution theorem we can obtain the solution for $W$

$$W(r,t) = \delta \int_0^t f(t-\tau) \left[ \frac{1}{\sqrt{\pi\tau}} \exp\left\{ \frac{-(r/a-1)^2}{4\alpha\tau} \right\} - \sqrt{\alpha} \exp\left\{ (r/a-1) + \alpha\tau \right\} \operatorname{erfc}\left\{ \frac{r/a-1}{2\sqrt{\alpha\tau}} + \sqrt{\alpha\tau} \right\} \right] d\tau$$

$$-\delta R \int_0^t f(t-\tau) \left[ \frac{1}{\sqrt{\pi\tau}} \exp\left\{ \frac{-(r/a-1)^2}{4\alpha R^2\tau} \right\} - \sqrt{\alpha} R \exp\left\{ (r/a-1) + \alpha R^2\tau \right\} \operatorname{erfc}\left\{ \frac{r/a-1}{2R\sqrt{\alpha\tau}} + R\sqrt{\alpha\tau} \right\} \right] d\tau \tag{55}$$

The pore pressure is

$$P(r,t) = \frac{W(r,t)}{r} \tag{56}$$

and the pore pressure evaluated at the surface of the waste package is

$$\lim_{r\to a} P(r,t) = \lim_{r\to a} \frac{W(r,t)}{r} = \frac{\delta}{a} \int_0^t f(t-\tau) \left[ \frac{1}{\sqrt{\pi\tau}} - \sqrt{\alpha} \exp\left\{ \alpha\tau \right\} \operatorname{erfc}\left\{ \sqrt{\alpha\tau} \right\} \right] d\tau$$

$$-\frac{\delta R}{a} \int_0^t f(t-\tau) \left[ \frac{1}{\sqrt{\pi\tau}} - \sqrt{\alpha} R \exp\left\{ R^2\alpha\tau \right\} \operatorname{erfc}\left\{ R\sqrt{\alpha\tau} \right\} \right] d\tau \tag{57}$$

With the pressure gradient, we can calculate the pressure-driven brine migration from (1). We first define

$$\xi = r/a$$

and write

$$v(\xi,t) = -\frac{k}{\mu}\frac{\partial P}{\partial r} = -\frac{k}{\mu}\left(\frac{1}{r}\frac{\partial W}{\partial r} - \frac{W}{r^2}\right) = -\frac{k}{\mu a^2}\left(\frac{1}{\xi}\frac{\partial W}{\partial \xi} - \frac{W}{\xi^2}\right) \tag{59}$$

Define

$$D(\xi,t) = \frac{1}{\sqrt{\pi t}}\exp\left\{\frac{-(\xi-1)^2}{4\alpha t}\right\} - \sqrt{\alpha}\exp\left\{(\xi-1)+\alpha t\right\}\operatorname{erfc}\left\{\frac{\xi-1}{2\sqrt{\alpha t}} + \sqrt{\alpha t}\right\}$$

$$-R\frac{1}{\sqrt{\pi t}}\exp\left\{\frac{-(\xi-1)^2}{4\alpha R^2 t}\right\} + \sqrt{\alpha}R^2\exp\left\{(\xi-1)+\alpha R^2 t\right\}\operatorname{erfc}\left\{\frac{\xi-1}{2R\sqrt{\alpha t}} + R\sqrt{\alpha t}\right\} \tag{60}$$

and the partial gradient of $D$ is

$$\frac{\partial D(\xi,t)}{\partial \xi} = -\frac{\xi-1}{2\alpha\sqrt{\pi t^3}}\exp\left\{\frac{-(\xi-1)^2}{4\alpha t}\right\} - \sqrt{\alpha}\exp\left\{(\xi-1)+\alpha t\right\}\operatorname{erfc}\left\{\frac{\xi-1}{2\sqrt{\alpha t}} + \sqrt{\alpha t}\right\}$$

$$+\frac{1}{\sqrt{\pi t}}\exp\left\{\frac{-(\xi-1)^2}{4\alpha t}\right\} + \frac{\xi-1}{2\alpha R\sqrt{\pi t^3}}\exp\left\{\frac{-(\xi-1)^2}{4\alpha R^2 t}\right\}$$

$$+\sqrt{\alpha}R^2\exp\left\{(\xi-1)+\alpha R^2 t\right\}\operatorname{erfc}\left(\frac{\xi-1}{2R\sqrt{\alpha t}} + R\sqrt{\alpha t}\right) - \frac{R}{\sqrt{\pi t}}\exp\left\{\frac{-(\xi-1)^2}{4\alpha R^2 t}\right\} \tag{61}$$

If we now define a $\Psi$ function as in (33) and (34), we have

$$\Psi(\xi,t) = -\frac{1}{\xi}\frac{\partial D}{\partial \xi} + \frac{D}{\xi^2} = \left(1-\frac{1}{\xi}\right)\frac{1}{2\alpha\sqrt{\pi t^3}}\left[\exp\left\{\frac{-(\xi-1)^2}{4\alpha t}\right\} - \frac{1}{R}\exp\left\{\frac{-(\xi-1)^2}{4\alpha R^2 t}\right\}\right]$$

$$-\frac{1}{\sqrt{\pi t}}\frac{1}{\xi}\left(1-\frac{1}{\xi}\right)\left[\exp\left\{\frac{-(\xi-1)^2}{4\alpha t}\right\} - R\exp\left\{\frac{-(\xi-1)^2}{4\alpha R^2 t}\right\}\right]$$

$$+\sqrt{\alpha}\frac{1}{\xi}\left(1-\frac{1}{\xi}\right)\left[\exp\{(\xi-1)+\alpha t\}\operatorname{erfc}\left\{\frac{\xi-1}{2\sqrt{\alpha t}} + \sqrt{\alpha t}\right\} - R^2\exp\left\{(\xi-1)+\alpha R^2 t\right\}\operatorname{erfc}\left\{\frac{\xi-1}{2R\sqrt{\alpha t}} + R\sqrt{\alpha t}\right\}\right] \tag{62}$$

Then we write the Darcian brine migration velocity as

$$v(\xi,t) = \frac{kb'\sqrt{\kappa}\theta_0}{\mu a^2(1-R^2)}\int_0^t f(t-\tau)\Psi(\xi,\tau)d\tau \tag{63}$$

Equation (63) can be used to compute brine flow near a waste package around which salt has fully consolidated.

## 3. Numerical Illustration

In this section we illustrate the above analytic solutions using parameters typical of a nuclear waste repository in salt. We use a waste sphere of radius 0.76 m in an infinite salt bed.

### 3.1 Temperature Profile

We consider a typical waste package containing spent fuel from pressurized water reactors.[8] This package contains 5.5 metric tons of uranium initially and has a thermal flux $Q_0$ of 928 watts per square meter of surface area initally. We approximate the normalized thermal flux, $f(t)$ in (4), using the data in Table 1, as

$$f(t) = e^{-0.024t} + e^{-0.0075t} + e^{0.0046t} - e^{0.0068t} - e^{-0.0073t} \tag{64}$$

Table II lists the material properties used in these numerical illustrations. Figure 2 shows the known time history of normalized thermal flux from the reference waste package and the fitted analytic expression.

Table 1. Relative Power of a Waste Package Containing Spent Fuel from PWR, 10 years out of reactor

| Years After Emplacement | Relative Power |
|---|---|
| 0 | 1.000 |
| 5 | 0.841 |
| 10 | 0.750 |
| 15 | 0.683 |
| 20 | 0.625 |
| 30 | 0.524 |
| 50 | 0.389 |
| 70 | 0.303 |
| 100 | 0.240 |
| 300 | 0.100 |
| 500 | 0.070 |
| 800 | 0.050 |
| 1000 | 0.045 |

Source: Reference 8.

Using the $f(t)$ thus obtained, we solve for the temperature field around the waste package as a function of radial distance and time. Figure 3 shows the temperature profile as a function of distance from the surface of the waste package 1 year, 10 years and 100 years after emplacement in salt. Because salt is a relatively good conductor of heat, the rise in temperature over the ambient decays rapidly. The time derivative of the relative temperature serves as the input and driving force for brine migration. Figure 4 shows the time history of relative temperature at the surface of the waste sphere. The maximum temperature is reached rapidly, although Figure 2 and 3 show that the thermal perturbation lasts for at least several hundred years.

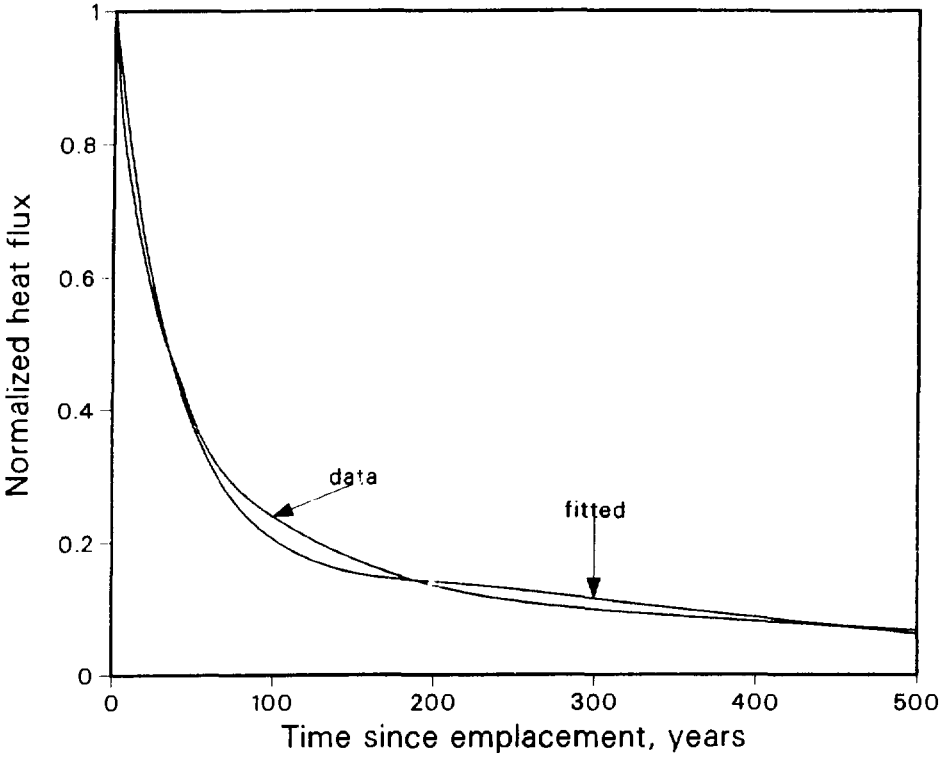


Figure 2. Comparison of Fitted versus Actual Heat Flux

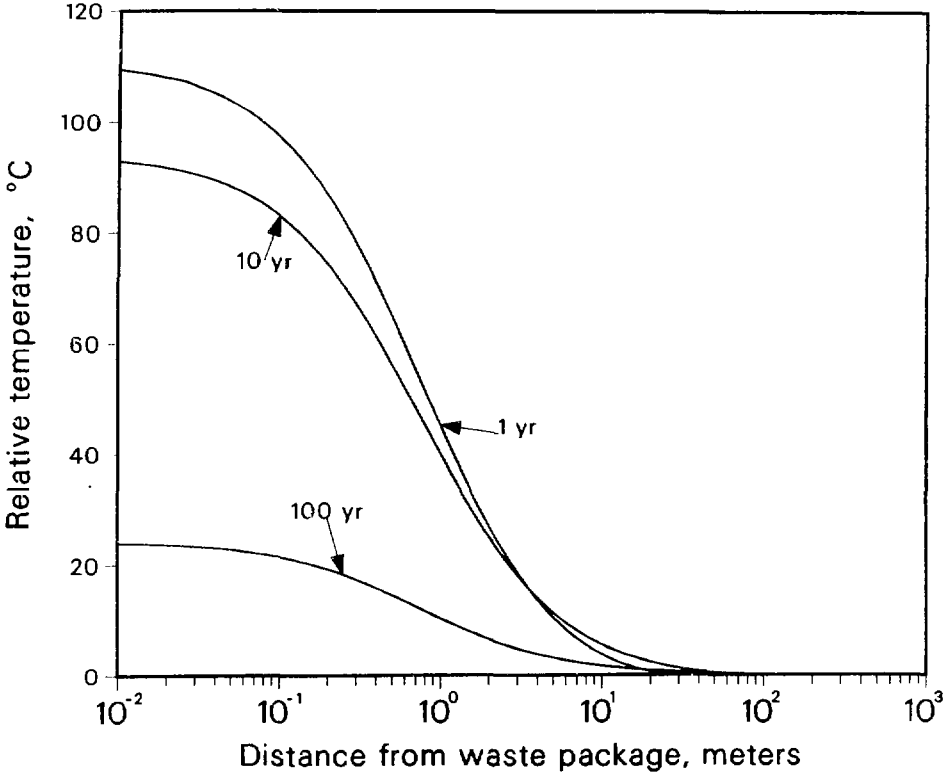


Figure 3. Relative Temperature in Salt After Emplacement

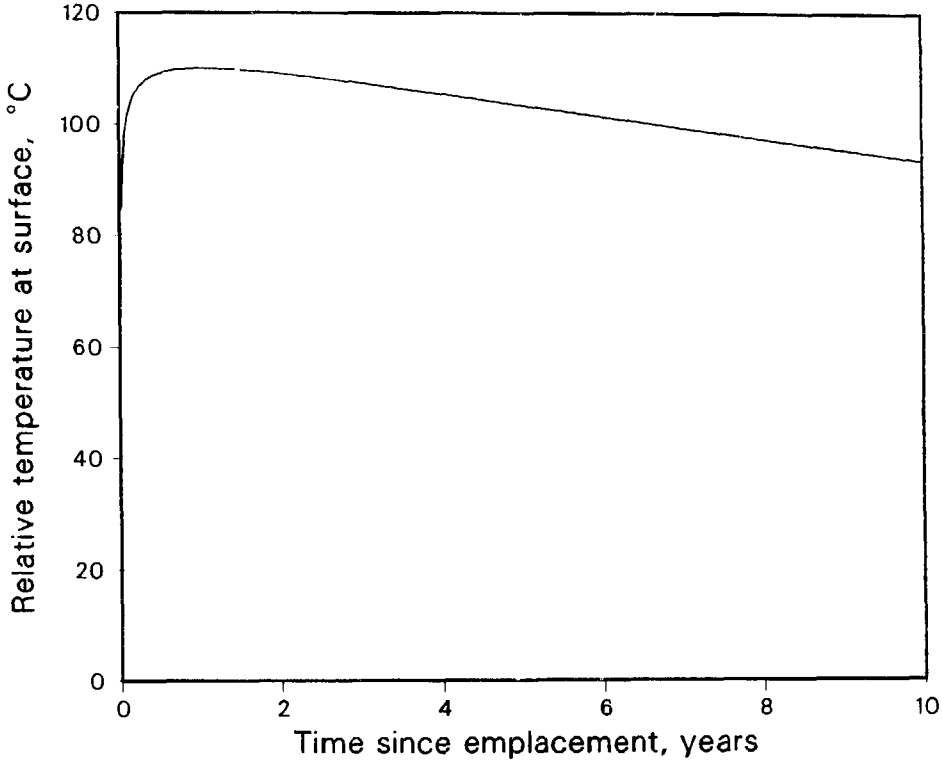


Figure 4. Relative Temperature at Waste Surface After Emplacement

Table II. Parameter Values Used in Calculations

(After McTigue,[2] for the Salado Formation, Delaware Basin, New Mexico)

| Property | Value | Units |
|---|---|---|
| Conductivity ($\lambda$) | 6.60 | W· m$^{-1}$·K$^{-1}$ |
| Heat Capacity ($\rho c_v$) | 1.89 x 10$^6$ | J· m$^{-3}$·K$^{-1}$ |
| Drained Bulk Modulus ($K$) | 20.7 | GPa |
| Fluid Bulk Modulus ($K_f$) | 2.0 | GPa |
| Solid Bulk Moduli ($K_s'$, $K_s''$) | 23.5 | GPa |
| Shear Modulus ($G$) | 12.4 | GPa |
| Porosity ($\phi_o$) | 0.001 | |
| Permeability ($k$) | $10^{-21}$ | m$^2$ |
| Fluid Expansivity ($\alpha_f$) | $3.0\times10^{-4}$ | K$^{-1}$ |
| Solid Expansivity ($\alpha_s'$, $\alpha_s''$) | $1.2\times10^{-4}$ | K$^{-1}$ |
| Fluid Viscosity ($\mu$) | 1.0 x 10$^{-3}$ | Pa· s |
| $B = \left\{1+\phi_o\frac{K(1-K_f/K'')}{K_f(1-K/K_s')}\right\}^{-1}$ | 0.93 | |
| Poisson's Ratio ($\nu$) | 0.25 | |
| Undrained Poisson's Ratio ($\nu_u$) | 0.27 | |
| $b'$, Eq. (2a) | 29.0 | kPa·K$^{-1}$ |
| Fluid Diffusivity ($c$) | 0.16 x 10$^{-6}$ | m$^2\cdot$s$^{-1}$ |
| Thermal Diffusivity ($\kappa$) | 3.5 x 10$^{-6}$ | m$^2\cdot$s$^{-1}$ |
| $R = \sqrt{c/\kappa}$ | 0.21 | |

### 3.2 Brine Migration into an Open Borehole

Using the analytic heat flux shown in Figure 2 and material properties of Table II, (35) is used to compute the velocity of brine migration into a borehole that has been kept open. The results for a spherical-equivalent waste package embedded in an infinite salt medium, using a permeability of $10^{-21}$ m$^2$, are shown in Figure 5. We assume a far-field brine pressure of lithostatic plus atmospheric ($p_o + 0.1$) of 16.3 MPa. It can be seen that the magnitude of brine inflow is small and that steady state is reached rapidly.

In the *Environmental Assessments*[9] of candidate salt repository sites, brine migration is predicted from an equation of the form derived for migration of brine inclusions under the influence of a temperature

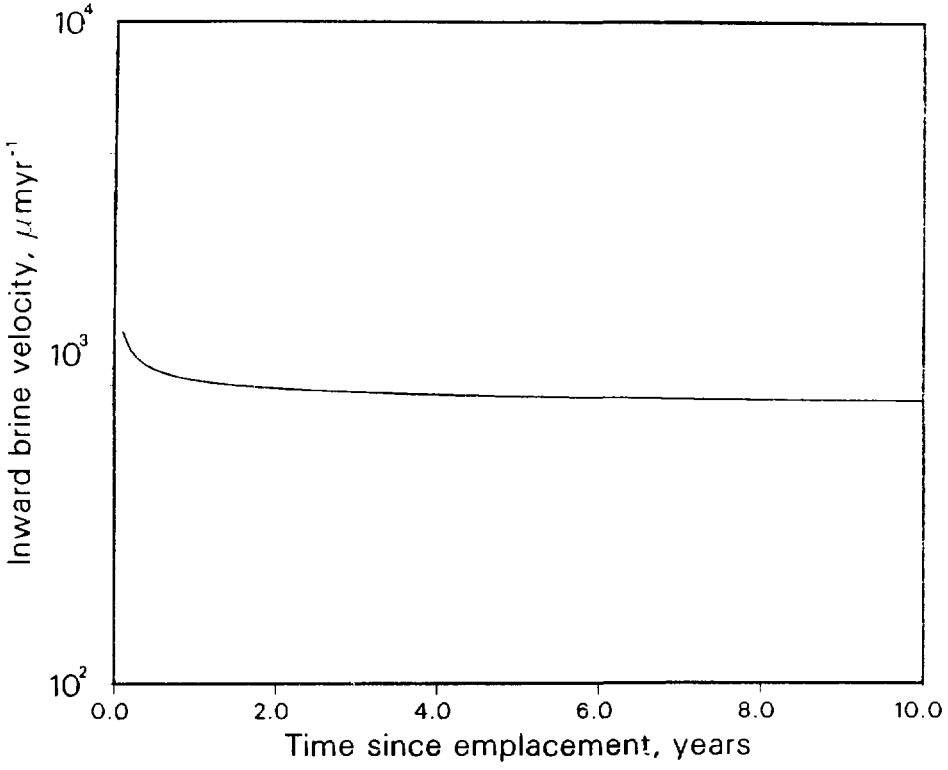


Figure 5. Inward Brine Migration Velocity into an Open Borehole

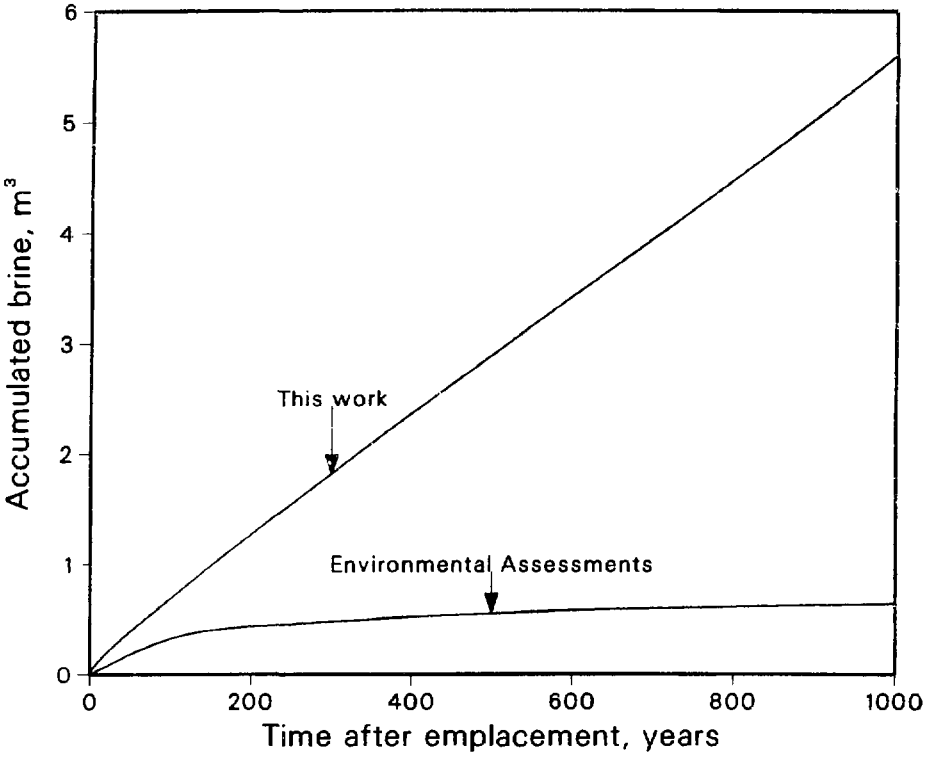


Figure 6. Brine Flow into an Open Borehole

gradient. Darcian flow is not included. In Figure 6 the *Environmental Assessments* prediction of cumulative brine inflow is shown along with our results for pressure-gradient flow, Case 1, Section 2.2. The calculated results are unrealistic for times greater than a few years, after which no open borehole is predicted to exist. However, results are calculated to 1000 years for a hypothetical open borehole, to compare with brine inflow calculations appearing in the *Environmental Assessments*. For the parameter values adopted herein, grain-boundary migration into an open borehole is driven almost entirely by the large difference between pressures in the far field and in the open borehole. For the long time scales of Figure 6, we calculate that brine will accumulate linearly with time. The *Environmental Assessments* incorrectly predict that brine accumulation is driven entirely by temperature gradients and reaches a constant value after the assumed effects of the thermal pulse have disappeared.

### 3.3 Brine Migration in Consolidated Salt

Equation (63) is used to compute brine migration velocity in salt consolidated around a waste package as a function of radial distance and time. In Figure 7 we plot the local brine pressure, relative to the far-field brine pressure, as a function of radial distance and time. After creep closes the annular space between the waste package and the emplacement hole wall, the pressure of brine rises above the far-field pressure because of thermal expansion of the hotter salt and brine. The built-up pressure relieves rapidly as brine flows outwards into cooler salt. In 100 years there is almost no pressure gradient and brine migration has become negligible. In 100 years the brine pressure in the immediate vicinity of the waste package is slightly less than the far-field brine pressure. At these times, brine will move toward the waste package.

Using the results shown in Figure 7 and the material properties in Table II, the Darcian brine migration velocity can be calculated. The results for 0.1 year, 1 year and 10 years are shown in Figure 8. The brine migration velocities are very low, of the order of microns per year. Brine flow is highly transient and is localized to the few meters of salt near the waste package. The maximum velocity occurs a few meters from the waste package and essentially disappears within ten years. Brine migration back towards the waste package occurs, but the reverse migration is weak and occurs at later time a few meters from the waste package.

To investigate the sensitivity of our results to uncertainty in material properties, we varied the permeability from $10^{-20}$ m$^2$/a to $10^{-22}$ m$^2$/a. The resultant brine migration velocities are shown in Figure 9. Although the permeability is varied a hundredfold, the peak velocity varies only fourfold.

Other material properties in Table II are uncertain and further sensitivity analysis can be done. For example, thermal conductivity is temperature dependent and experimental results at the same temperature varies substantially. The National Bureau of Standards[10] recommends a value of 6.57 W$\cdot$ m$^{-1}\cdot$K$^{-1}$ at 300 K and 4.80 W$\cdot$ m$^{-1}\cdot$K$^{-1}$ at 400 K. The elastic properties of salt shown in Table II are from extensive measurements

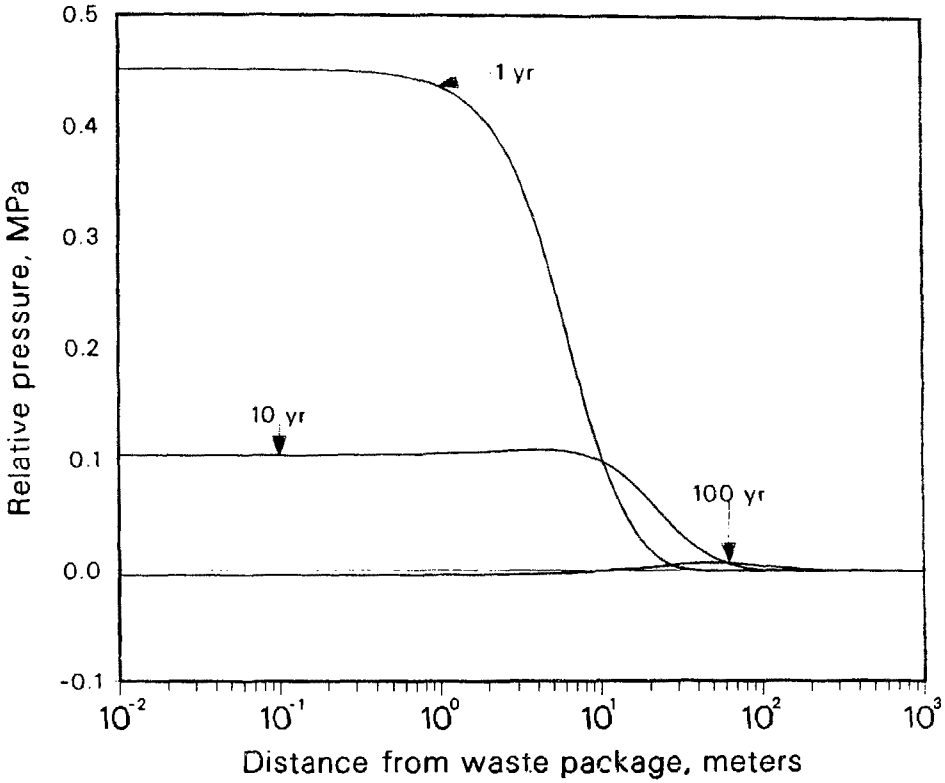


Figure 7. Pressure Profile in Consolidated Salt

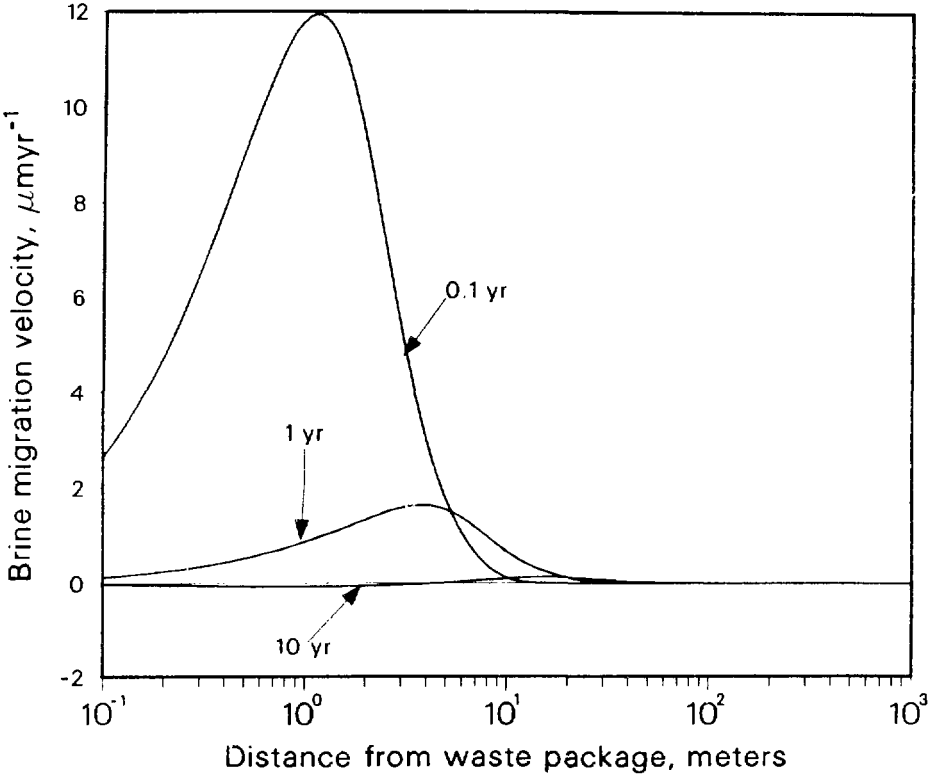


Figure 8. Darcian Brine Migration Velocity in Consolidated Salt

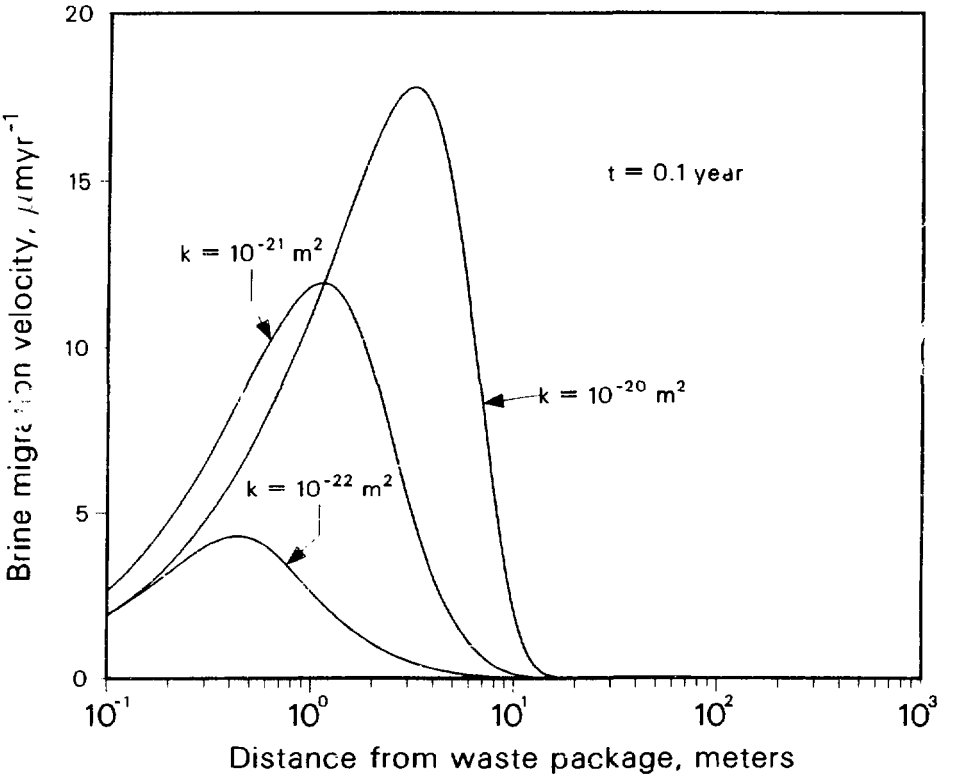


Figure 9. Sensitivity of Brine Migration Velocity to Salt Permeability

of salt properties at the Waste Isolation Pilot Plant and are quite reliable. The viscosity of brine is probably twice that of pure water, or $2 \times 10^{-3}$ Pa·s, but is a sharper function of temperature. These variations in parameter values may have offsetting effect on the overall analysis.

## 4. Comparison of Advective and Diffusive Radionuclide Transport

In this section we compare the rate of mass transport by advection with the rate by diffusion.[11] The mass rate of advective transport at location $r$ from a spherical surface and at time $t$ is given by

$$\dot{m}_a(r,t) = 4\pi\epsilon r^2 v_p N(r,t) \tag{65}$$

where $\dot{m}_a$ is the mass rate of advective transport [M/t],

$v_p$ is the pore brine migration velocity, $v_p = v/\epsilon$ [L/t] from section 3.3, and

$N(r,t)$ is the species concentration at position $r$ and time $t$ [M/L$^3$].

To obtain an estimate for $N(r,t)$, we use the result from diffusive transport analysis. This assumes that the rate of advective transport by brine migration is small compared to the transport rate by diffusion through the brine.

The mass rate of diffusion is given by

$$\dot{m}_d(r,t) = -4\pi\epsilon r^2 D \frac{\partial N(r,t)}{\partial r} \tag{66}$$

where $\dot{m}_d$ is the mass rate of diffusion [M/t],

$D$ is the species diffusion coefficient [L$^2$/t].

For long-lived solubility-limited species the diffusion-controlled concentration is given by

$$N(r,t) = \frac{N^* r_o}{r} \mathrm{erfc}\left\{\frac{(r-r_o)}{2}\sqrt{K/Dt}\right\}, \qquad r > r_o, \quad t > 0 \tag{67}$$

where $K$ is the species retardation coefficient, and

$N^*$ is the solubility of the species [M/L$^3$].

In Figure 10 we show the absolute value of the mass transport rates as predicted by advective brine migration and by molecular diffusion as a function of distance from the waste surface, for 10 years and 100 years. For this comparison we use $\epsilon = 0.001, D = 10^{-11}$ m$^2$/s, $N^* = 10^{-3}$ g/m$^3$, and $K = 1$. The advective flux at 10 and 100 years are actually *negative*. Figure 10 shows that for the parameters selected here, the mass transport rate by diffusion is always higher than the mass transport rate by advection.

Figure 11 shows the flux comparison at one year. At one year the advective flux is positive, but its magnitude is smaller than the diffusive flux.

The above results can be understood through Figure 12 where we show on a non-dimensionalized basis the concentration profile as predicted by the diffusive analysis and the brine migration velocity, at ten years.

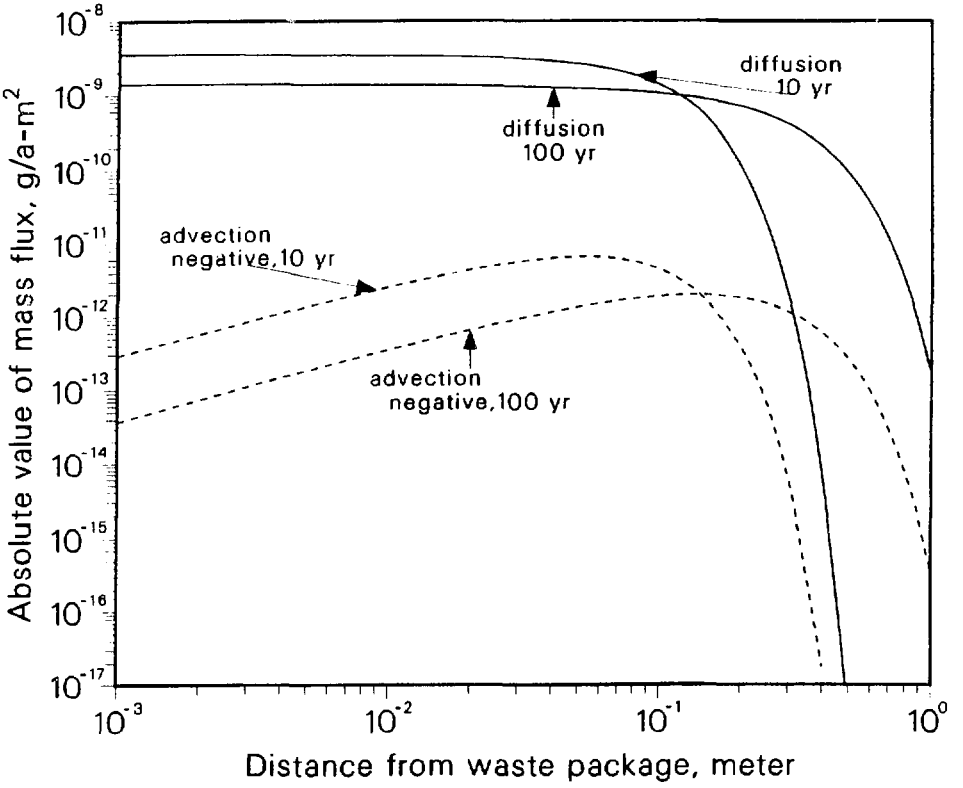


Figure 10. Mass Flux Rate by Advection and Molecular Diffusion

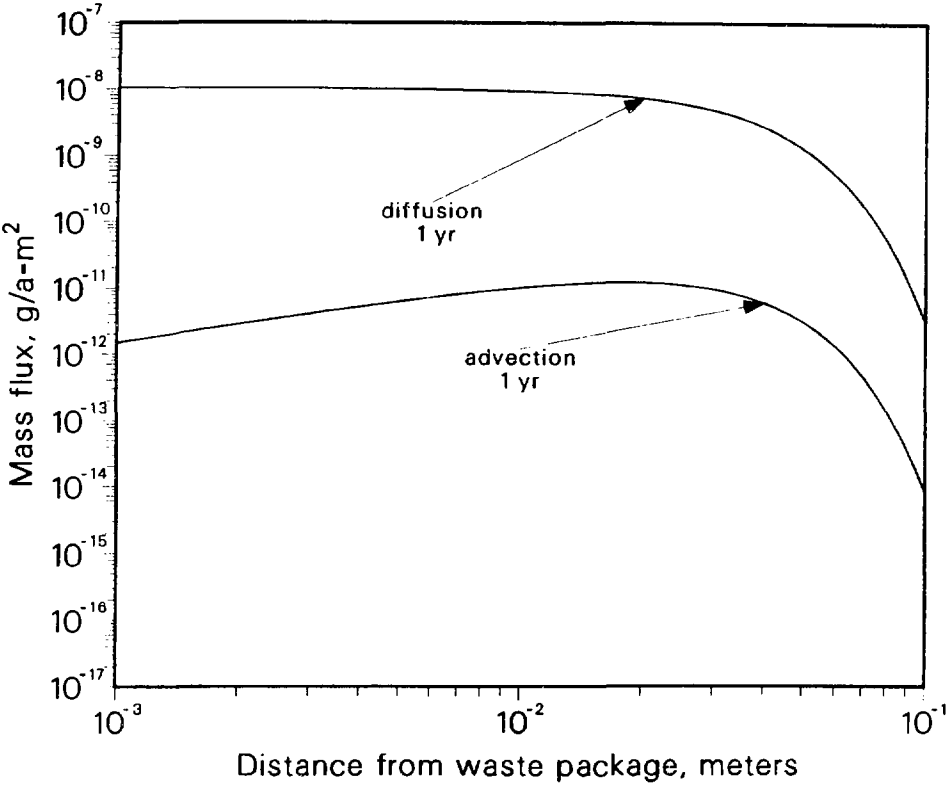


Figure 11. Comparison of Mass Flux Rate at Early Time

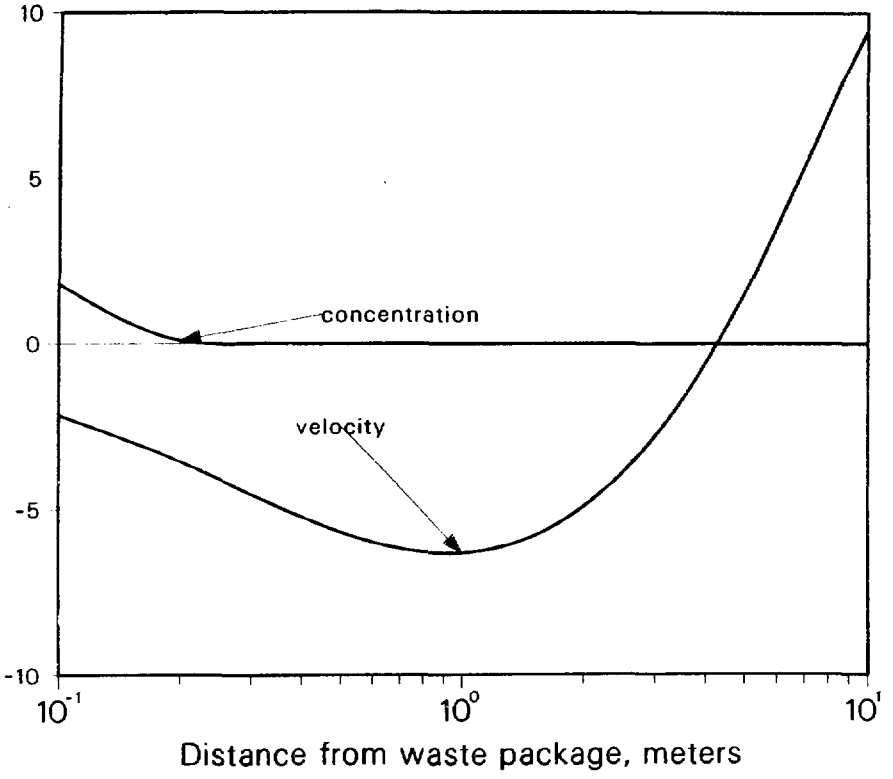


Figure 12. Relative Concentration and Velocity at Ten Years Since Emplacement

The advective mass flux is proportional to the product of these two curves. The brine velocity is negative in the immediate vicinity of the waste surface. Hence the product of the concentration and the migration velocity is negative, making the mass flux negative. However, this negative mass flux does not occur at the surface of the waste.

## 5. Conclusions

We present in this report an analysis of pressure-driven brine migration in salt. We consider a high-level waste package emplaced in a borehole in salt and backfilled with salt. After few years later salt has consolidated around the waste package. After consolidation brine migration analysed by these equations and using the particular set of parameter values is of a small magnitude, with Darcy velocities of the order of microns per year. Advective transport of dissolved contaminants by brine migration is slow compared to diffusive transport in consolidated salt. Brine migration in consolidated salt is very localized, within a few meters from the waste package, and highly transient, fading to even lower velocities within about ten years.

Therefore, we conclude that in geologic repositories of nuclear waste where salt creep is expected to consolidate around high-level waste packages within a few years after emplacement, pressure-driven brine migration appears not to be important in determining compliance with U. S. Nuclear Regulatory Commission's release rate requirement.[12] For the purpose of determining release rates it appears realistic to apply previously developed analytical tools for analyzing releases from waste packages in salt repositories.[13] We have published such results[14] and a report on that subject is published separately.[11]

## References


1. J. D. Bredehoeft, "Will Salt Repositories Be Dry?" *Eos, 69,* 121, 1988.
2. D. F. McTigue, "Thermoelastic Response of Fluid-Saturated, Porous Rock," *J. Geophy. Res., 91, B9,* 9533, 1986.
3. T. Brandshaug, *Estimate of Consolidation of Crushed Salt Around a Spent Fuel Waste Package,* RE/SPEC Report RSI-315, 1987.
4. T. H. Pigford and P. L. Chambré, "Mass Transfer in a Salt Repository," Report LBL-19918, 1985.
5. Y. Hwang, P. L. Chambré, W. W.-L. Lee and T. H. Pigford, "Pressure-Induced Brine Migration into an Open Borehole in a Salt Repository," *Trans. Am. Nuc. Soc., 55,* 133, 1987.
6. Y. Hwang, P. L. Chambré, W. W.-L. Lee and T. H. Pigford, "Pressure-Induced Brine Migration in Consolidated Salt in a Repository," *Trans. Am. Nuc. Soc., 55,* 132, 1987.
7. J. Cossar and A. Erdelyi (compilers), *Dictionary of Laplace Transforms,* London, Admiralty Computing Service, Department of Scientific Research and Experiment, 1944.
8. Westinghouse, *Waste Package Reference Conceptual Design for a Repository in Salt,* Report ONWI-517, 1986.
9. U.S. Department of Energy, *Environmental Assessment, Deaf Smith County Site, Texas,* DOE/RW-0069, 1986.
10. L. H. Gevantman (ed.). *Physical Properties Data of Rock Salt,* National Bureau of Standards Mono-

graph 167, 1981.

11. Y. Hwang, P. L. Chambré, T. H. Pigford and W. W.-L. Lee, *Radionuclide Release Rates in Salt by Diffusion*, Report LBL-25767, 1988.

12. U. S. Nuclear Regulatory Commission, Disposal of High-Level Radioactive Wastes in Geologic Repositories, 10 *Code of Federal Regulations* 60.113(a)(1)(ii)(B).

13. T. H. Pigford and P. L. Chambré, "Radionuclide Transport in Geologic Repositories: A Review," in M. J. Apted and R. E. Westerman (eds.), *Scientific Basis for Nuclear Waste Management XI*, Pittsburgh, Materials Research Society, 125, 1988.

14. P. L. Chambré, Y. Hwang, W. W.-L. Lee and T. H. Pigford, "Release Rates from Waste Packages in a Salt Repository," *Trans. Am. Nuc. Soc.*, *55*, 131, 1987.